

***Baccharis trimera* (Less.) DC: An Innovative Cardioprotective Herbal Medicine Against Multiple Risk Factors for Cardiovascular Disease**

Marília Moraes Queiroz Souza,¹ Gustavo Ratti da Silva,¹ Itaruã Machri Cola,¹ Anieli Oliveira Silva,²
Maysa Isernhagen Schaedler,² Lucas Pires Guarnier,² Rhanany Alan Calloi Palozi,² Lorena Neris Barboza,¹
Jacqueline Vergutz Menetrier,¹ Diego Lacir Froelich,³ Pablo Alvarez Auth,¹ Alan de Almeida Veiga,⁴
Lauro Mera de Souza,⁴ Evelylyn Claudia Wietzikoski Lovato,¹ João Tadeu Ribeiro-Paes,⁵
Arquimedes Gasparotto Junior,² and Francislaine Aparecida dos Reis Lívero¹

¹Laboratory of Preclinical Research of Natural Products, Postgraduate Program in Medicinal Plants and Phytotherapeutics in Basic Attention, Paranaense University, Umuarama, Paraná, Brazil.

²Laboratory of Electrophysiology and Cardiovascular Pharmacology, Faculty of Health Sciences, Federal University of Grande Dourados, Dourados, Mato Grosso do Sul, Brazil.

³Laboratory Prevention and Diagnosis, Assis Gurgacz Faculty, Cascavel, Paraná, Brazil.

⁴Institute of Research Pelé Pequeno Príncipe, Pequeno Príncipe Faculty, Curitiba, Paraná, Brazil.

⁵Laboratory of Genetics and Cell Therapy, São Paulo State University, UNESP, Assis, São Paulo, Brazil.

ABSTRACT Cardiovascular disease (CVD) is the leading cause of death worldwide and among its modifiable risk factors are dyslipidemia, diabetes, and smoking. Experimental models evaluated this risk factors singly, however, there is a lack of models that agglomerate these risk factors, resembling real patients and elucidating the pathophysiology of CVD. Moreover, few studies have investigated the cardioprotective effects of *Baccharis trimera*, a species with lipid-lowering effects. In this study, ethanol-soluble fraction of *B. trimera* was characterized by liquid chromatography–mass spectrometry. Diabetes was induced by streptozotocin in Wistar rats that also received 0.5% cholesterol-enriched chow and were exposed to the smoke of nine cigarettes, 5 days/week, for 4 weeks. During the last 2 weeks, the animals were treated with vehicle (C⁻), *B. trimera*, or simvastatin plus insulin. At the end, cholesterol, triglyceride, urea, and creatinine levels; blood pressure (BP); heart rate (HR); abdominal aortic morphometry; vascular reactivity; renal and cardiac oxidative status; and histopathological changes were evaluated. The agglomerate of risk factors promoted alterations contrary to those described in the literature for the isolated risk factors. The C⁻ group exhibited oxidative stress, increase in biochemical parameters, and thickening of the wall of the abdominal aorta. HR, systolic, diastolic, and mean BP decreased, and vascular reactivity was altered. Cardiac and renal histopathological changes were observed. Treatment with *B. trimera* reversed these changes and this effect may be partially attributable to lipid-lowering action and to the inhibition of free radical generation. *B. trimera* has cardioprotective effects in this model, with no toxicity.

KEYWORDS: • *carqueja* • *diabetes mellitus* • *dyslipidemia* • *herbal medicine* • *rats* • *smoking*

INTRODUCTION

ACCORDING TO THE World Health Organization, more people die annually from cardiovascular disease (CVD) than from any other disease, making CVD the leading cause of death worldwide. By 2015, ~17.7 million people died

from CVD (31% of all deaths globally), with the highest occurrence (75%) in low- and middle-income countries.¹

Two main risk factors are associated with CVD: (1) nonmodifiable risk factors (*e.g.*, sex, age, and heritability/genetics) and (2) modifiable risk factors that are acquired over time and are related to inadequate living habits (*e.g.*, smoking, sedentary lifestyle, stress, obesity, hypertension, diabetes mellitus, and dyslipidemia).² Most animal studies of these risk factors have been performed in an isolated way (*i.e.*, studies of individual risk factors rather than combinations of risk factors). However, modifiable risk factors often occur concomitantly. Previous epidemiological studies

Manuscript received 02 August 2019. Revision accepted 21 September 2019.

Address correspondence to: Francislaine Aparecida dos Reis Lívero, PhD, Laboratory of Preclinical Research of Natural Products, Paranaense University, Praça Mascarenhas de Moraes, 4282, P.O. Box 224, Umuarama 87502-210, Paraná, Brazil, E-mail: francislaine@prof.unipar.br

indicated the occurrence of two or more risk factors for CVD in up to 54% of patients.³ Thus, designing studies that evaluate combinations of risk factors is fundamental because the presence of more than one risk factor for CVD is associated with a higher risk than any one risk factor alone, thus indicating synergistic effects of these risk factors.⁴

Given the high morbidity and mortality of CVD, new therapeutic agents need to be developed with greater efficacy and fewer side effects. One promising therapy is treatment with the species *Baccharis trimera*, popularly known as “carqueja,” which is used for its hepatoprotective and hypocholesterolemic effects.^{5,6} This species exerts antioxidant actions through the scavenging of reactive oxygen and nitrogen species and increasing activity of the antioxidant system. Hepatoprotective, anti-inflammatory, hypoglycemic, and lipid-lowering effects of this plant have also been reported.^{5–7}

However, its cardiovascular effects are still unknown. Thus, the present study investigated the cumulative effects of multiple modifiable risk factors, including dyslipidemia, diabetes, and smoking, on the development of CVD and the cardioprotective effects of *B. trimera* in this experimental model.

MATERIALS AND METHODS

B. trimera extract preparation and phytochemical analysis

Aerial parts of *B. trimera* were collected in February 2018 in the Medicinal Plants Garden of the Paranaense University (UNIPAR), which is located 430 m above sea level (S23°46'11.3"–W53°16'41.2"). A voucher specimen (no. 07) was deposited in the herbarium of UNIPAR. The soluble ethanol fraction was prepared according to previously described methods⁸ and the extract yield was 16.88%. The phytochemical analysis was carried out in an ultra-performance liquid chromatography (UPLCTM, Acquity, Waters) coupled to a high-resolution mass spectrometry (HR-MS—Xevo, Waters), equipped with a BEH C18 (Waters), 50×2.1 mm and 1.7 μm of particle size, operating at 40°C.

The separation was performed in a gradient mode, with ultrapure water (MilliQ-Millipore) and acetonitrile (Merck-Sigma), acidified with 0.1% of formic acid. The solvent gradient was developed at 400 μL/min, initiating with acetonitrile at 5%, held for 1 min, then increasing to 30% in 7 min and to 95% in 15 min. The initial condition (5% acetonitrile) returned at 16 min, and 2 min were spent to re-equilibrate the column (total run time of 18 min).

The compounds were detected in the negative and positive ion mode, MSe centroid. However, most of the components were better detected in the negative ionization. The analysis was carried out with source temperature held at 150°C, desolvation at 350°C using nitrogen at a flow rate of 50 L/H in the cone, and 500 L/H for the sample desolvation. The energies for positive ionization were: 3 kV in the capillary, 30 V in the cone, and 60 V in the source offset, and for negative ionization, the energies were: 3 kV, 40 V, and 80 V, respectively. The mass range was 100–1400 *m/z*, and the

fragmentation was produced by a ramp of collision energy, from 30 to 50 V, and the mass range. Mass correction was performed by internal calibration with leu-enkephalin, *m/z* 556.2771, 278.1141 [M]⁺ and *m/z* 554.2615, 236.1035 [M][–].

Experimental animals

Male Wistar rats, weighing 200–250 g, were housed at a temperature of 20°C±2°C with 50%±10% relative humidity under a 12-h light/12-h dark cycle. The experimental protocol was approved by the Committee for Ethics in Research Involving Animal Experimentation, UNIPAR (protocol no. 1000/2018). The study was conducted and described in accordance with the ARRIVE Guidelines.⁹

Experimental design and treatments

After a 12-h fast, the animals received 60 mg/kg streptozotocin, diluted in citrate buffer (10 mM, pH 4.5, i.p.). Three days later, glycemia was measured with a glucose meter in a small volume of peripheral blood that was collected from the tail. Rats with glycemia ≥250 mg/dL were considered diabetic. For the induction of dyslipidemia, the diabetic animals received a standard diet that was enriched with 0.5% cholesterol *ad libitum* for 4 weeks.¹⁰

Concomitantly, the animals were exposed to nine commercial tobacco cigarettes (0.8 mg nicotine, 10 mg tar, and 10 mg carbon monoxide) for 1 h/day, 5 days/week.¹¹ During the last 2 weeks, the animals were treated once daily by gavage with vehicle (filtered water, negative control [C[–]] group), *B. trimera* extract (30, 100, and 300 mg/kg), or simvastatin (2.5 mg/kg) plus insulin (6 IU, subcutaneously; SIM+INS group). In parallel, normoglycemic, nondyslipidemic, and nonsmoke-exposed rats that were treated with vehicle served as the basal group.

Analysis of hemodynamic parameters

At the end of treatments, the animals were intramuscularly anesthetized with ketamine (100 mg/kg) and xylazine (20 mg/kg). The left carotid artery was cannulated and connected to a pressure transducer that was coupled to a computerized recording system to measure systolic, diastolic, and mean blood pressure (BP) and heart rate (HR) for 20 min.

Arterial ultrasonography and vascular reactivity

The rats were intraperitoneally anesthetized with ketamine (80 mg/kg) and xylazine (20 mg/kg). The animals were then placed in the dorsal decubitus position for ultrasonography (Mindray M5 device, 7 Hz linear transducer). Afterward, the mesenteric vascular bed was isolated as described by Schaedler *et al.*¹² Changes in perfusion pressure (mmHg) were measured by a pressure transducer that was connected to a pressure recording system.

For this, mesenteric vascular beds were placed in a water-jacketed organ bath and perfused with physiological saline solution (PSS, NaCl 119 mM; KCl 4.7 mM; CaCl₂ 2.4 mM; MgSO₄ 1.2 mM; NaHCO₃ 25.0 mM; KH₂PO₄

1.2 mM; dextrose 11.1 mM; and EDTA 0.03 mM) at 37°C and gassed with 95% O₂/5% CO₂. After 30 min, mesenteric vascular beds were continuously perfused with phenylephrine (3 nmol) to induce a prolonged increase in perfusion pressure and acetylcholine (30 pmol) to evaluate decrease in perfusion pressure. An equilibration period (15 min) was allowed between each drug administration.

Sample collection for biochemical and histopathological analyses

After a 12-h fast, blood was collected from the ocular plexus to evaluate plasma levels of cholesterol, triglycerides, urea, and creatinine. Samples of the heart and kidneys were collected to evaluate the antioxidant system based on superoxide dismutase (SOD) activity and reduced glutathione (GSH) and lipoperoxidation (LPO) levels.^{13–15}

For the histopathological analysis, samples of the aortic artery and heart were collected, fixed in paraformaldehyde, sectioned, and stained with Hematoxylin and Eosin. The slides were analyzed by a veterinarian pathologist by optical microscopy. The wall thickness of the arteries was measured, and the values are expressed as pixels. Myocardial lesions were classified as the following: 0 (no alterations), 1 (mild; focal myocyte damage or small multifocal degeneration with a slight degree of an inflammatory process), 2 (moderate; extensive myofibrillar degeneration and/or a diffuse inflammatory process), and 3 (accentuated; necrosis with a diffuse inflammatory process).¹⁶

Statistical analyses

Data were analyzed for homogeneity of variance and a normal distribution. One-way analysis of variance (ANOVA) followed by the Newman–Keuls *post hoc* test was used. Values of $P < .05$ were considered statistically significant.

RESULTS

Compounds present in ethanol-soluble fraction of *B. trimer*a

The phytochemicals observed in the negative ionization liquid chromatography–mass spectrometry, were mainly composed by polar phenolics (Fig. 1A–E), although the first peak observed on the chromatogram (0.38 min) was consistent with quinic acid, at m/z 191.0633. The series of chlorogenic acids was also observed, however, the monocaffeoylquinic acids (m/z 353.08) appeared at a lower concentration than the dicaffeoylquinic acids (m/z 515.11). The monocaffeoyl quinic acids were classified according to their differences in the fragmentation profiles, as *neo*-chlorogenic acid (1.30 min), chlorogenic acid (2.53 min), and *crypto*-chlorogenic acid (2.99 min). Similarly, differences in the MS² profiles were useful to differentiate the dicaffeoylquinic acids, as 3,4-di-*O*-caffeoylquinic acid (5.54 min), 3,5-di-*O*-caffeoylquinic acid (5.61 min, Fig. 1D), and 4,5-di-*O*-caffeoylquinic acid (6.01 min). Despite the presence of those cinnamoylquinic acids, the most

abundant peaks on the chromatogram of the ethanol-soluble fraction of *B. trimer*a were identified as flavonoids, mainly apigenin-*C*-glycosides, along with a methyl-apigenin. The peak at 4.04 min, at m/z 593.1544 produced a characteristic fragmentation profile (Fig. 1B), with sequential neutral losses (NL) of 90 and 120 atomic mass units (a.m.u.). This fragmentation profile arising from the ^{0,2}X and ^{0,3}X cleavages, on hexopyranosyl rings, being consistent with the apigenin-6,8-di-*C*-glucopyranoside (Vicenin 2). Three other *C*-glycoside isomers were found at m/z 563.138 (4.35, 4.53, and 4.76 min) producing very similar fragments with losses of 90 and 120 a.m.u. These isomers were consistent with apigenin-*C*-hexoside-*C*-pentoside, similar to the isomers of Vicenin 1 and 3 (Fig. 1C). Furthermore, the main peak on the chromatogram, observed at 9.80 min, gave the negative ion at m/z 283.0612. This ion is consistent with the methoxylated aglycone, apigenin, but the fragments from this negative ion (m/z 268.0375 and 161.0235) were poorly informative, just confirming the loss of a radical methyl (CH₃[•]—NL 15.0237 a.m.u.). Thus, this compound was also analyzed in the positive ionization, giving rise to the ion at m/z 285.0749 [M+H]⁺, yielding the fragments at m/z 270.0500[•], 242.0553[•], 167.0349, and 124.0108[•] (Fig. 1E). The fragments with an even m/z value are characteristics of the loss of the methyl group (CH₃[•]) by homolytic cleavage, yielding radical fragments. Similar fragments were observed from acacetin (4'-*O*-Me-apigenin). The fragment at m/z 133.0649 was described as arising from B-ring of acacetin that are methoxylated, thus its absence could indicate an isomer of acacetin, methoxylated in a different site. Moreover, the fragment at m/z 153.0183 was replaced, here, by that one at m/z 167.0349, 14 a.m.u. higher, confirming the methyl group attached to the A-ring, in *O*-5 or *O*-7, similar to the Genkwanin (7-Me-Apigenin). Two peaks gave negative ions at m/z 349.2021 (8.67 min) and m/z 333.2072 (10.81 min), respectively. Both ions did not produce fragments hindering their identification. However, the elementary compositions obtained based on mass spectra were C₂₀H₂₉O₄ and C₂₀H₂₉O₅. These seem to be the acidic forms of the lactone, diterpene clerodane, which was described in *B. trimer*a (Torres *et al.*, 2000¹⁷; Garcia *et al.*, 2014¹⁸). The results are summarized in Table 1.

*B. trimer*a reverses the decreases in HR and BP

A decrease in HR was observed in the C⁻ group compared with the basal group. *B. trimer*a (30 and 100 mg/kg) normalized HR. Treatment with SIM+INS was ineffective (Fig. 2A). Decreases in mean BP (Fig. 2B), systolic BP (Fig. 2C), and diastolic BP (Fig. 2D) were observed in the negative control group (C⁻). Treatment with *B. trimer*a (30 mg/kg) and SIM+INS effectively reversed these changes.

*B. trimer*a reverses thickening of the arterial wall and recovers vascular reactivity

An increase in the wall thickness was observed in the C⁻ group. *B. trimer*a and SIM+INS effectively reversed this

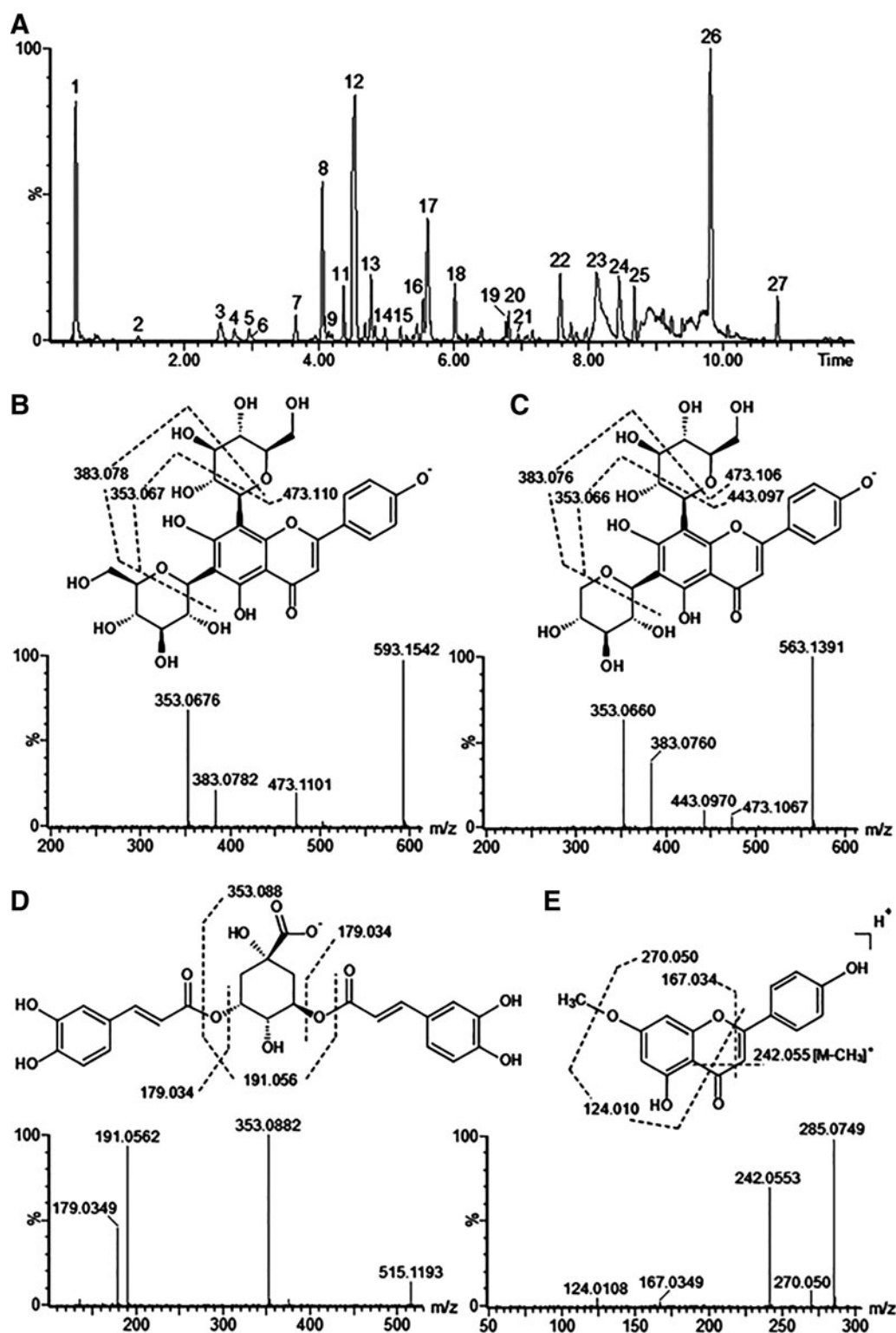


FIG. 1. Phytochemical analysis of the ethanol-soluble fraction of *Baccharis trimera* extract by LC-MS (A) and the fragmentation profile and cleavages of the main peaks on the chromatogram. (B) Mass spectrum and tentative structure from the peak 8, identified as Vicenin 2, (C) from the peak 12, identified as Vicenin 1 or 3, (D) from the peak 17—3,5-Dicafeoylquinic acid and (E) from the peak 26, identified as a 7-(or 5)-methylapigenin. LC-MS, liquid chromatography coupled to a mass spectrometry.

TABLE 1. PHYTOCHEMICAL COMPOSITION FROM THE ETHANOL SOLUBLE FRACTION OF *BACCHARIS TRIMERA* EXTRACT OBTAINED BY LIQUID CHROMATOGRAPHY COUPLED TO A MASS SPECTROMETRY ANALYSIS

Peak	tR	MS ¹⁻	MS ²⁻	Tentative structures
1	0.38	191.0633	—	Quinic acid
2	1.30	353.0872	191.0546, 179.0332, 135.0473	neo-Chlorogenic acid
3	2.53	353.0869	191.0552	Chlorogenic acid
4	2.74	179.0345	135.0439	Caffeic acid
5	2.96	367.1037	193.0503, 173.0449, 134.0372	3-O-Feruloylquinic acid
6	2.99	353.0876	191.0532, 179.0329, 173.0441, 135.0437	crypto-Chlorogenic acid
7	3.65	447.1518	401.1458, 269.1033, 161.0454	n.i.
8	4.04	593.1542	473.1101, 383.0782, 353.0676	Apigenin-6,8-di-C-glucoside
9	4.13	367.1022	191.0551	4-O-Feruloylquinic acid
10	4.18	367.1021	193.0495, 173.0456	5-O-Feruloylquinic acid
11	4.35	563.1382	473.1054, 443.0990, 383.0759, 353.0657	Apigenin-C-pentoside-C-hexoside
12	4.53	563.1391	473.1067, 443.0970, 383.0760, 353.0660	Apigenin-C-pentoside-C-hexoside
13	4.76	563.1385	473.1036, 443.0957, 383.0774, 353.0649	Apigenin-C-pentoside-C-hexoside
14	4.82	529.1328	367.1022, 193.0508	Feruloyl-caffeoylquinic acid
15	4.96	483.1303	173.0450, 163.0450	di-O-p-coumaroylquinic acid
16	5.54	515.1187	353.0891, 191.0554, 179.0343, 173.0453	3,4-di-O-caffeoylquinic acid
17	5.61	515.1193	353.0882, 191.0562, 179.0349	3,5-di-O-caffeoylquinic acid
18	6.01	515.1174	353.0879, 191.0552, 179.0349, 173.0453	4,5-di-O-caffeoylquinic acid
19	6.76	529.1342	367.1005, 193.0433, 173.0449	Feruloylcaffeoylquinic acid
20	6.81	971.4384	631.3338	n.i.
21	6.95	839.3929	631.3337	n.i.
22	7.58	661.3644	—	n.i.
23	8.12	703.3735	—	n.i.
24	8.45	841.4037 ²⁻	—	n.i.
25	8.67	349.2021	—	Clerodane derivative
26	9.8	283.0612	268.0375, 161.0235	5/7-methyl-apigenin
		285.0749	270.0500, 242.0553, 167.0349, 124.0108	
27	10.81	333.2072	—	Clerodane derivative

tR, retention time; n.i., not identified.

thickening (Fig. 3B, C). With regard to vascular reactivity, phenylephrine infusion increased perfusion pressure in the C⁻ group (Fig. 3D). The infusion of acetylcholine decreased perfusion pressure in the C⁻ group (Fig. 3E). Treatment with *B. trimera* (30 and 100 mg/kg) effectively reversed these changes, whereas SIM+INS treatment only reversed the increase in BP that was induced by phenylephrine.

B. trimera reverses plasma lipid changes, renal marker damage, and oxidative stress

Increases in plasma levels of glucose, cholesterol, triglycerides, urea, and creatinine were observed in the C⁻ group. *B. trimera* and SIM+INS effectively reversed these lipid alterations. Only *B. trimera* at 30 and 100 mg/kg effectively reversed renal damage. An increase in cardiac LPO, a decrease in GSH levels, and a decrease in SOD activity were observed in the C⁻ group. These alterations were completely reversed by *B. trimera* and partially reversed by SIM+INS. The same pattern of LPO and GSH changes observed in the heart also occurred in the kidney, except by SOD, since there were no changes between groups (Table 2).

B. trimera reverses cardiac and renal histopathological damage. No microscopic changes were observed in the kidneys or hearts in the basal group (Fig. 4A, E). In the

kidneys, moderate multifocal degeneration of the proximal convoluted tubules and mild multifocal hemorrhage and swelling of the tubular cells were observed in the C⁻ group (Fig. 4B). Treatment with 30 mg/kg *B. trimera* reversed these alterations (Fig. 4C). In the C⁻ group, the cardiac lesion score was 3 (Fig. 4F). Treatment with 30 mg/kg *B. trimera* reversed these alterations to a score of 1 (Fig. 4G). Treatment with *B. trimera* at doses of 100 and 300 mg/kg was less effective, which resulted in cardiac lesion scores of 2 and 3, respectively. Treatment with SIM+INS reversed these alterations (Fig. 4D, H).

DISCUSSION

This study evaluated the effects of multiple cardiovascular risk factors, including diabetes mellitus, dyslipidemia, and smoking, in a rat model of CVD. Most previous studies evaluated individual risk factors in isolation. The synergistic effects of these multiple risk factors differ from the simple sum of the effects of individual risk factors, as reported in current scientific literature.

One issue is whether the present experimental model indeed generated atherosclerosis. Arterial ultrasonography is routinely used in clinical practice and has been validated as a screening method for atherosclerosis. The present model resulted in thickening of the aortic arterial wall, thus confirming the atherogenic potential of the model. This result

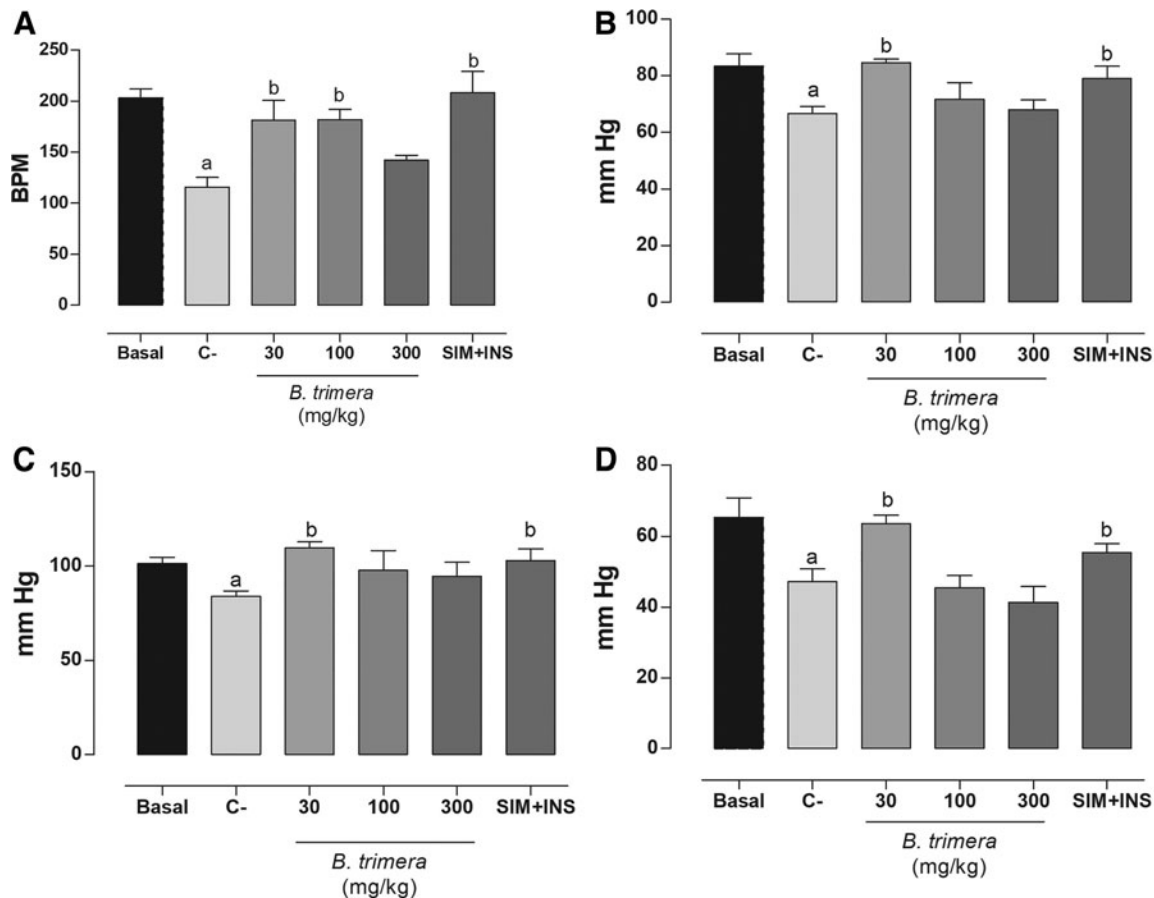


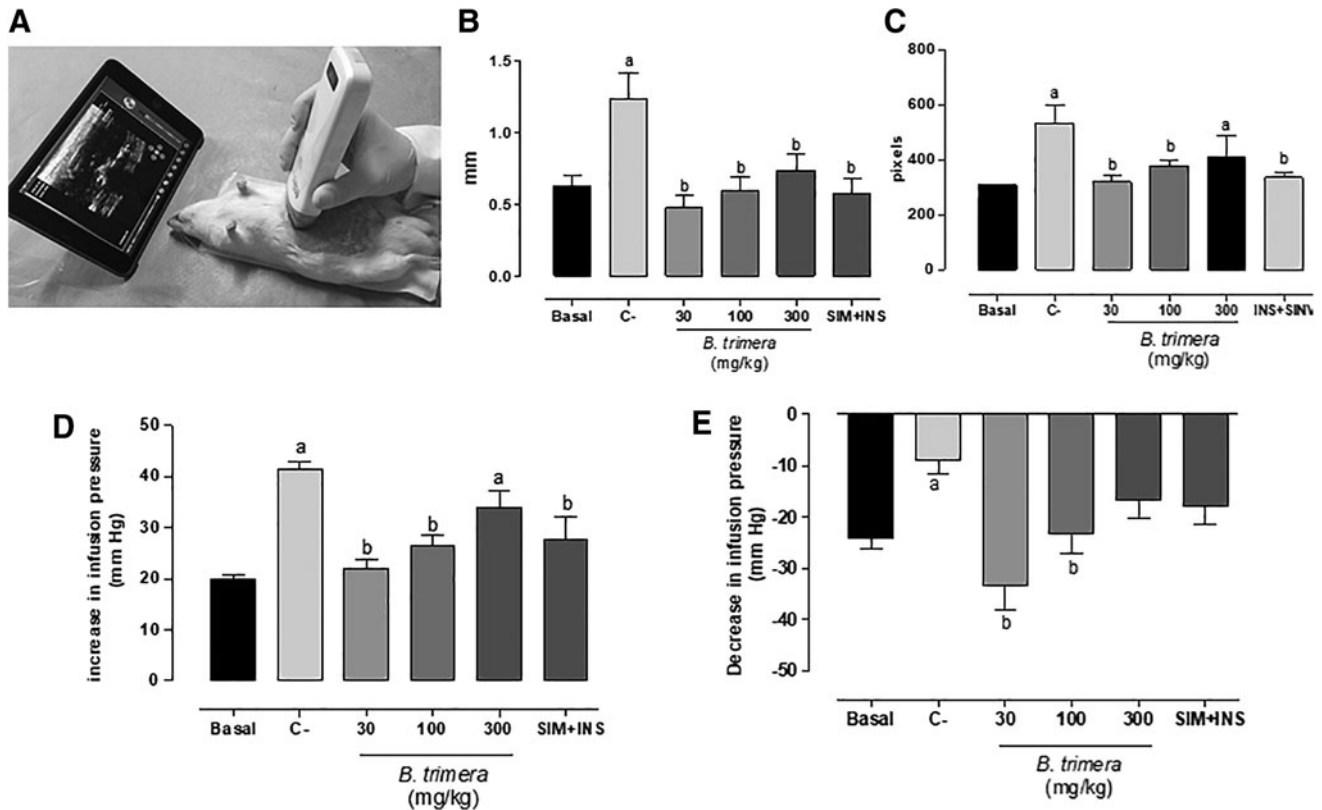
FIG. 2. (A) HR (BPM), systolic BP (B), diastolic BP (C), and mean BP (D) in normoglycemic, nondyslipidemic, and nonsmoker Wistar rats (basal group) and diabetic, dyslipidemic, and smoker Wistar rats that were treated with vehicle (C-), *B. trimera* (30, 100, and 300 mg/kg), or SIM+INS. Data are expressed as mean \pm SEM. ^a $P < .05$, versus C- group; ^b $P < .05$, versus C+ group (one-way ANOVA followed by Newman-Keuls *post hoc* test). ANOVA, analysis of variance; BP, blood pressure; BPM, beats per minute; HR, heart rate; SIM+INS, simvastatin+insulin.

was confirmed by histopathological measurements of the arterial wall. Walker *et al.*¹⁹ correlated the wall thickness of the carotid arteries, visualized by ultrasound and histologically, and concluded that the imaging method was highly sensitive, with good correspondence between the two methods. Another indirect sign of endothelial dysfunction that was generated by the model was the increase in perfusion pressure in the analysis of vascular reactivity with adrenaline in the mesenteric bed and the reduction of the vasodilator response with acetylcholine. Ambrose and Barua²⁰ evaluated both animal and human models and stated that the failure of vasodilator function is one of the earliest signs of the establishment of atherosclerosis, which results from a decrease in the bioavailability of nitric oxide.

Significantly higher serum levels of total cholesterol and triglycerides were observed compared with previous studies that employed hypercholesterolemic diets. Dinh *et al.*²¹ subjected rats to a high-fat diet and measured BP and serum triglyceride and total cholesterol levels. Increases in triglycerides and total cholesterol were found, which is consistent with the present study, but no changes in BP were

observed. This absence of BP changes is in contrast to the present study, in which we found decreases in both BP and HR. This suggests that dyslipidemia may reflect the body's response to a high-fat diet, but it may be associated with either normal or high BP.²¹

Talukder *et al.*²² and Nemmar *et al.*²³ exposed rats to cigarette smoke and observed significant increases in BP but no changes in HR. The literature shows some clear examples of the relationship between smoking and BP, in which the inhalation of tobacco smoke increases BP. This finding is well established but differs from the present findings. Smoking may compromise cardiac function, independent of coronary disease, through cardiac remodeling. Talukder *et al.*²² reported an increase in BP in rats that were exposed to cigarette smoke, with an increase in left ventricular mass and no increase in body weight. In previously hypertensive rats, exposure to cigarette smoke significantly accelerated the progression of cardiac hypertrophy. This latter finding supports the present results, suggesting that the decrease in BP resulted from the development of heart failure and demonstrating synergism between smoking and other associated risk factors.



Diastolic dysfunction in diabetic cardiomyopathy may precede systolic dysfunction. Calligaris *et al.*²⁴ reported that β-adrenergic stimulation is compromised in cardiomyocytes that accumulate lipids, leading to a decrease in HR. Considering the pathophysiology of cardiac dys-

function that is generated by smoking and diabetes, these two risk factors appear to converge on the same final pathway to synergistically potentiate cardiac fibrosis, resulting in global cardiac dysfunction and decreases in BP and HR.

TABLE 2. BIOCHEMICAL PROFILE OF DIABETIC, DYSLIPIDEMIC, AND SMOKER WISTAR RATS THAT WERE TREATED WITH VEHICLE, *BACCHARIS TRIMERA*, AND SIM+INS

	Basal	C ⁻	Baccharis trimera			SIM+INS
			30	100	300	
Glucose	87.1 ± 4.1	515.7 ± 28.1 ^a	478.6 ± 15.1 ^a	556.1 ± 11.4 ^a	430.4 ± 28.6 ^{ab}	213.0 ± 114.2 ^{ab}
Cholesterol	79.73 ± 6.4	1776.0 ± 178.9 ^a	180.5 ± 26.3 ^b	411.3 ± 69.4 ^{ab}	750.4 ± 45.1 ^{ab}	85.84 ± 11.2 ^b
Triglycerides	55.77 ± 14.1	1476.0 ± 215.7 ^a	204.1 ± 34.1 ^b	276.5 ± 66.2 ^b	432.7 ± 154.3 ^b	129.4 ± 45.9 ^b
Urea	33.87 ± 3.5	69.83 ± 8.2 ^a	44.10 ± 7.3	50.57 ± 8.8	75.10 ± 11.7 ^a	68.78 ± 7.2 ^a
Creatinine	0.24 ± 0.02	0.50 ± 0.13 ^a	0.24 ± 0.02 ^b	0.20 ± 0.01 ^b	0.35 ± 0.07	0.31 ± 0.02
LPO-heart	77.9 ± 7.4	210.5 ± 10.3 ^a	69.3 ± 7.6 ^b	94.7 ± 3.1 ^b	126.1 ± 12.6 ^{ab}	87.8 ± 4.7 ^b
GSH-heart	168.5 ± 24.7	67.86 ± 9.1 ^a	243.7 ± 34.9 ^b	178.4 ± 29.4 ^b	141.9 ± 19.3	92.03 ± 17.2
SOD-heart	1554.0 ± 38.9	1294.0 ± 32.6 ^a	1493.0 ± 64.2	1326.0 ± 36.3 ^a	1333.0 ± 30.9 ^a	1344.0 ± 50.1 ^a
LPO-kidney	65.4 ± 5.2	117.5 ± 12.1 ^a	78.6 ± 2.4 ^b	84.3 ± 2.2 ^b	96.6 ± 3.7 ^{ab}	85.9 ± 1.5 ^b
GSH-kidney	127.6 ± 16.4	61.7 ± 9.3 ^a	117.9 ± 19.3 ^b	82.8 ± 15.5 ^b	63.2 ± 12.6 ^a	103.1 ± 7.1 ^b
SOD-kidney	858.1 ± 18.9	931.9 ± 11.8	915.3 ± 10.8	962.1 ± 17.1	947.3 ± 21.9	933.3 ± 15.6

^a*P* < .05 versus basal; ^b*P* < .05 versus C⁻.

Glucose, cholesterol, triglycerides, urea and creatinine were performed in plasma and are expressed as mg/dL.

C⁻, negative control; GSH, reduced glutathione (μg GSH/g of tissue); LPO, lipoperoxidation (nmol/min/g of tissue); SIM+INS, simvastatin+insulin; SOD, superoxide dismutase (U SOD/g of tissue).

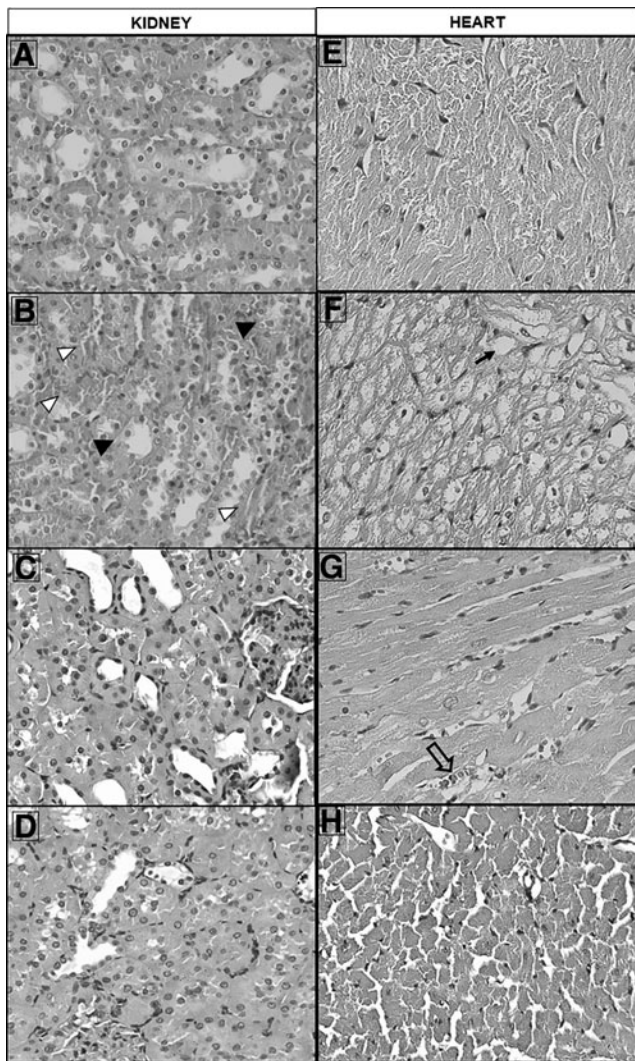


FIG. 4. Renal and cardiac histopathological analysis of (A, E) normoglycemic, nondyslipidemic, and nonsmoker Wistar rats (basal group, negative control) and diabetic, dyslipidemic, and smoker Wistar rats that were treated with (B, F) vehicle (C^- group, positive control), (C, G) *B. trimera* extract (30 mg/kg), and (D, H) SIM+INS. The black arrow indicates fatty vacuoles within myocytes. The open arrow indicates multifocal vacuolar congestion. The black arrowhead indicates moderate multifocal degeneration of proximal tubules. The white arrowhead indicates mild multifocal hemorrhage.

B. trimera reversed all of the changes that were observed in the present experimental model of CVD. This extract reversed abdominal wall thickening of the abdominal aorta at the three doses tested. The lowest dose exerted effects that were comparable to SIM+INS. The increase and decrease in perfusion pressure in the mesenteric bed were normalized only by the 30 and 100 mg/kg doses of *B. trimera*. No difference was found between SIM+INS and the highest dose (300 mg/kg) of *B. trimera*. The normalization of pressure levels was achieved only by treatment with SIM+INS and *B. trimera* at the lowest dose tested (30 mg/kg). The reversal of HR to normal levels occurred only with the 30 and

100 mg/kg doses of *B. trimera*, with no effect of the SIM+INS or highest dose (300 mg/kg). The absence of results with highest dose of *B. trimera* is justified based on “inverted U effect.” In fact, in the evaluation of crude extracts, where there are many secondary metabolites acting independently (on different targets), synergistically, or antagonistically, this effect is quite common. Normally, what is expected of a substance (or all of them) is that it has a dose where its maximum effect is reached. From this dose, there is no point in increasing the dose because there is no additional therapeutic gain, a phenomenon known as plateau. This dose–response curve usually occurs because the maximum effect of that biological tissue or organic function has already been reached.

Lívero *et al.*⁵ reported a decrease in plasma triglyceride and total cholesterol levels in a model of alcoholic liver steatosis in mice that were treated with *B. trimera* (30 mg/kg/day). No previous studies of which we are aware have evaluated the effects of *B. trimera* on vascular reactivity, HR, or arterial wall thickening. Rabelo and Costa⁶ reviewed the literature on the pharmacological and biological activity of this species. These authors stated that the plant has antioxidant activity that is exerted by flavonoids and phenolic compounds, which upregulate activity of the antioxidant enzyme system and sequester reactive oxygen species. These actions may intercept many pathways that are involved in the pathophysiological mechanisms that are described in the atherosclerotic process, thus conferring cardioprotective activity to *B. trimera* that has not been previously described. In the present study, treatment with *B. trimera* reversed the imbalance of redox status in animals that were subjected to multiple risk factors.

There are several justifications that arouse the interest of further cardiovascular studies on *B. trimera*. Its lipid-lowering activity may reduce the production of fat by the liver from excess glucose, thus reducing the genesis and progression of atherosclerosis. Hyperglycemia, in addition to obesity, can cause important endothelial damage. *B. trimera* also exerts antioxidant effects that are related to both cardioprotective and renoprotective actions. This species has been reported to have no toxic effects.^{6,7} Interestingly, in the present study, the lowest dose of *B. trimera* presented better therapeutic activity than the higher doses. Such a finding may arouse interest within the pharmaceutical industry to industrialize and commercialize this plant, making it an important therapeutic agent for the treatment of CVD that is associated with multiple risk factors.

The synergistic effects of multiple risk factors for CVD appear to be much more aggressive than simply the sum of effects of individual risk factors. *B. trimera* was shown to be an effective cardiovascular protective agent in the present experimental model.

ACKNOWLEDGMENTS

The authors thank Dalton Leonardo Mello, Danilo Adriato, Dirce Consuelo, Gislayne Marcelino, Jennifer Rezende, Jordana dos Reis, Larissa Pereira, Luana Meirinho,

Nathan Varago, Rafael dos Santos, Raquel Stramazo, Rebeca Matos, and Thais Fugisawa de Freitas for help with the experiments and Michael Arends for proofreading the article.

AUTHOR DISCLOSURE STATEMENT

No competing financial interests exist.

FUNDING INFORMATION

This research was supported by Diretoria Executiva de Gestão da Pesquisa e da Pós-Graduação (DEGPP, UNIPAR) and Fundação de Apoio ao Desenvolvimento do Ensino, Ciência e Tecnologia do Estado de Mato Grosso do Sul (FUNDECT, no. 59/300351/2016).

REFERENCES

- World Health Organization: *Global Atlas on Cardiovascular Disease Prevention and Control*. World Health Organization, Geneva 2011.
- Azevedo TA, Moreira MLV, Nucera APCS: Cardiovascular risk estimation by the ASCVD risk estimator application in a university hospital. *Int J Cardiovasc Sci* 2018;31:492–498.
- Pereira JC, Barreto SM, Passos VMA: Cardiovascular risk profile and health self-evaluation in Brazil: A population-based study. *Rev Panam Salud Publica* 2009;25:491–498.
- Mamudu HM, Alamina A, Paul T, *et al.*: Diabetes, subclinical atherosclerosis and multiple cardiovascular risk factors in hard-to-reach asymptomatic patients. *Diab Vasc Dis Res* 2018;15: 519–527.
- Lívero FAR, Martins GC, Telles JEJ, *et al.*: Hydroethanolic extract of *Baccharis trimera* ameliorates alcoholic fatty liver disease in mice. *Chem Biol Interact* 2016;260:22–32.
- Rabelo ACS, Costa DC: A review of biological and pharmacological activities of *Baccharis trimera*. *Chem Biol Interact* 2018; 296:65–75.
- Lívero FAR, Silva LM, Ferreira DM, *et al.*: Hydroethanolic extract of *Baccharis trimera* promotes gastroprotection and healing of acute and chronic gastric ulcers induced by ethanol and acetic acid. *Naunyn Schmiedebergs Arch Pharmacol* 2016; 389:985–998.
- Barboza LN, Lívero FAR, Prando TBL, *et al.*: Atheroprotective effects of *Cuphea carthagenensis* (Jacq.) J.F. Macbr. in New Zealand rabbits fed with cholesterol-rich diet. *J Ethnopharmacol*. 2016;187:134–145.
- Kilkenny C, Browne WJ, Cuthill IC, *et al.*: Improving bioscience research reporting: The ARRIVE guidelines for reporting animal research. *PLoS Biol* 2010;8:e1000412.
- Jaldin RG, Filho HAF, Sequeira JL, Yoshida WB: The atherosclerotic process in rabbit arteries submitted to low cost experimental egg yolk supplemented diet (Portuguese). *J Vasc Bras* 2006;5:247–256.
- Cakir Y, Yang Z, Knight CA, *et al.*: Effect of alcohol and tobacco smoke on mtDNA damage and atherogenesis. *Free Radic Biol Med* 2007;43:1279–1288.
- Schaedler MI, Palozi RAC, Tirloni CAS, *et al.*: Redox regulation and NO/cGMP plus KC channel activation contributes to cardiorenal protection induced by *Cuphea carthagenensis* (Jacq.) J.F. Macbr. in ovariectomized hypertensive rats. *Phytomedicine* 2018; 51:7–19.
- Jiang ZY, Hunt JV, Wolff SP: Ferrous ion oxidation in the presence of xylenol orange for detection of lipid hydroperoxide in low density lipoprotein. *Analytical Biochem* 1992;202:384–389.
- Sedlak J, Lindsay RH: Estimation of total, protein-bound, and nonprotein sulfhydryl groups in tissue with Ellman's reagent. *Analytical Biochem* 1968;25:192–205.
- Gao R, Yuan Z, Zhao Z, Goa X: Mechanism of pyrogallol autoxidation and determination of superoxide dismutase enzyme activity. *Bioelectrochem Bioenerg* 1998;45:41–45.
- Filho HGL, Ferreira NL, Sousa RB, Carvalho ER, Lobo PLD, Filho JGL: Experimental model of myocardial infarction induced by isoproterenol in rats. *Rev Bras Cir Cardiovasc* 2011;26:469–476.
- Torres LM, Gamberini MT, Roque NF, Lima-Landman MT, Souccar C, Lapa AJ: Diterpene from *Baccharis trimera* with a relaxant effect on rat vascular smooth muscle. *Phytochemistry* 2000;55:617–619.
- Garcia FAO, Tanae MM, Torres LMB, Lapa AJ, Lima-Landman MTR, Souccar C: A comparative study of two clerodane diterpenes from *Baccharis trimera* (Less.) DC on the influx and mobilization of intracellular calcium in rat cardiomyocytes. *Phytomedicine* 2014;21:1021–1025.
- Walker M, Campell BR, Azer K, *et al.*: A novel 3-dimensional micro-ultrasound approach to automated measurement of carotid arterial plaque volume as a biomarker for experimental atherosclerosis. *Atherosclerosis* 2009;204:55–65.
- Ambrose JA, Barua RS: The pathophysiology of cigarette smoking and cardiovascular disease: An update. *J Am Coll Cardiol* 2004;43:1731–1737.
- Dinh QN, Chrissobolis S, Diep H, *et al.*: Advanced atherosclerosis is associated with inflammation, vascular dysfunction and oxidative stress, but not hypertension. *Pharmacol Res* 2017;116: 70–76.
- Talukder MAH, Johnson WM, Varadharaj S, *et al.*: Chronic cigarette smoking causes hypertension, increased oxidative stress, impaired NO bioavailability, endothelial dysfunction, and cardiac remodeling in mice. *AM J Physiol Heart Circ Physiol* 2011;300:H388–H396.
- Nemmar A, Raza H, Subramanian D, *et al.*: Short-term systemic effects of nose-only cigarette smoke exposure in mice: Role of oxidative stress. *Cell Physiol Biochem* 2013;31:15–24.
- Calligaris SD, Lecanda M, Solis F, *et al.*: Mice long-term highfat diet feeding recapitulates human cardiovascular alterations: An animal model to study the early phases of diabetic cardiomyopathy. *PLoS One* 2013;8:e60931.